Resonance Prediction for Closed and Open Wind Tunnel by the Finite-Element Method

In Lee*
Stanford University, Stanford, California

A finite-element approach is developed for predicting the so-called "resonant" frequencies of subsonic wind tunnels with variously shaped cross sections. The resulting computer code has been applied to various wind tunnels. For example, the resonant frequencies for both the NASA Ames Research Center 6 ft × 6 ft wind tunnel (rectangular cross section) and the NASA Langley Research Center 16 ft × 16 ft transonic dynamics tunnel (octagonal cross section) have been calculated. The resonant frequencies of a wind tunnel with one slot are much smaller than those of a wind tunnel with many slots at the same open ratio. The results are believed to be more accurate than theoretical values used in the past for an equivalent rectangular cross section.

Nomenclature

a_0 = speed of sound of fluid medium
a_e = effective speed of sound of fluid medium defined in Eq. (16)
$\boldsymbol{B}$ = work function on boundary
$\boldsymbol{B}_c$ = complementary work function on boundary
$[B]$ = matrix defined in Eq. (38)
d = width of slot
e = slot open area ratio
F = variational functional for complementary system
H = height of tunnel
i = $\sqrt{-1}$
$[K]$ = stiffness matrix for whole system
$[k]$ = element stiffness matrix
L = Lagrangian function
M = freestream Mach number
$[m]$ = element mass matrix
$[M]$ = mass matrix for whole system
$\lfloor N \rfloor$ = row matrix of shape function
p = perturbation pressure
$\{\boldsymbol{p}\}$ = column vector of nodal pressure values
S = boundary surface
T = kinetic energy
$\boldsymbol{T}_c$ = complementary kinetic energy
t = time
U = freestream velocity
U = potential energy
U_c = complementary potential energy
V = volume
x, y, z = rectangular coordinates
α = wave number
α_f = nondimensional resonant frequency
β = $\sqrt{1-M^2}$
ξ = acoustic displacement
ρ = density in undisturbed stream
ϕ = perturbation velocity potential in test section
ω = angular frequency

Presented as Paper 86-0898 at the AIAA/ASME/ASCE/AHS 27th Structures, Structural Dynamics, and Materials Conference, San Antonio, TX, May 19–21, 1986; received Feb. 23, 1987; revision received Jan. 29, 1988.

*Graduate Student, Department of Aeronautics and Astronautics; currently Assistant Professor, Department of Mechanical Engineering, Korea Advanced Institute of Science and Technology. Member AIAA.

I. Introduction

THERE is considerable interest in the use of wind tunnels for dynamic experiments such as flutter test and unsteady wing and control surface airload measurements. The results of these tests will be affected by the so-called "resonance" problem when the model frequency is near a wind-tunnel resonant frequency. The results under such a coincidence in frequencies could be in considerable error, relative to free flight in the flutter testing of an aeroelastic model and other unsteady testing.[1,2]

Tunnel resonance is defined as an acoustic phenomenon that occurs when a disturbance from the oscillating wing is reflected from the tunnel wall back to the wing with such a phase relationship that it reinforces succeeding disturbances.[4] This behavior was predicted theoretically by several investigators.[3–7] The analysis of Refs. 3–5 refers to two-dimensional wings in closed tunnels and employs the method of images to satisfy the tunnel wall boundary conditions. Acum studied this problem by a simplified approach.[6] Other prior investigators have obtained the resonant frequencies for a two-dimensional tunnel or a tunnel with a rectangular cross section. However, it is difficult to predict analytically the frequencies for an arbitrarily shaped cross section. In such an instance, the finite-element method is a powerful alternative.

II. Governing Equation and Boundary Condition

If we consider a rectangular coordinate system defined as shown in Fig. 1, then for small disturbances the perturbation velocity potential satisfies the following equation:

$$(1-M^2)\phi_{zz}+\phi_{xx}+\phi_{yy}-(2M^2/U)\phi_{zt}-(M^2/U^2)\phi_{tt}=0 \quad (1)$$

Many wind tunnels have a number of slots running parallel to the axis of the tunnel to reduce the model blockage effect. Transonic slots on the wind tunnel wall are shown schematically in Fig. 1.

It is well known[3] that the boundary condition at a solid wall is $\partial\phi/\partial n = 0$. The pressure outside the wall is assumed equal to the freestream pressure. The perturbation pressure at a slot is assumed to be very small, and the boundary condition at a slot is assumed to be equivalent to $\phi = 0$. Many investigators use the foregoing boundary condition ($\phi = 0$) at a slot in accordance with the usual practice in tunnel-interference theory.[6,9] At the edge of the slot, the boundary condition changes from $\partial\phi/\partial n = 0$ to $\phi = 0$. Also, it should be noted that the boundary

condition ($\phi = 0$ at a slot) is very much idealized, and it would be desirable to simulate the free boundary condition more accurately. The flow in the absence of a model is given by $\phi = 0$ everywhere. However, it is necessary to obtain nonzero oscillatory solutions of Eq. (1) satisfying the same boundary conditions in order to solve the resonance problem.

We assume disturbances of the form

$$\phi = \phi_R = \Phi(x, y)e^{i\alpha z}e^{i\omega t} \tag{2}$$

where Φ is any function of x and y, and α is a streamwise wave number. Substituting Eq. (2) into Eq. (1), we get

$$\Phi_{xx} + \Phi_{yy} + \left[\frac{\omega^2 M^2}{U^2} + \frac{2M^2\omega\alpha}{U} - (1 - M^2)\alpha^2\right]\Phi = 0 \tag{3}$$

The boundary condition on the solid wall is given as

$$\frac{\partial \Phi}{\partial n} = 0 \tag{4}$$

where n is the outward normal to the boundary, and on the open wall it is given as

$$\Phi = 0 \tag{5}$$

The following procedure to derive the resonance condition is repeated from Ref. 6 for an easy understanding of resonance phenomena. Equation (3) can be written as

$$\Phi_{xx} + \Phi_{yy} + \Lambda^2\Phi = 0 \tag{6}$$

Equation (6) with the boundary conditions (4) and (5) has a nontrivial solution if Λ has one of the eigenvalues Λ_n ($n = 1,2,...$)

$$\Lambda_n^2 = (\omega^2 M/U^2) + (2M^2\omega\alpha/U) - (1 - M^2)\alpha^2 \tag{7}$$

Rearranging this equation, we get

$$\beta^2\alpha^2 - (2M^2\omega/U)\alpha - [(\omega^2 M^2/U^2) - \Lambda_n^2] = 0 \tag{8}$$

Then

$$\beta^2\alpha = (M^2\omega/U) \pm [(M^2\omega^2/U^2) - \beta^2\Lambda_n^2]^{1/2} \tag{9}$$

When

$$(M\omega/U) \geq \beta\Lambda_n \tag{10}$$

α has real values, and Eq. (2) represents a traveling wave of constant amplitude.

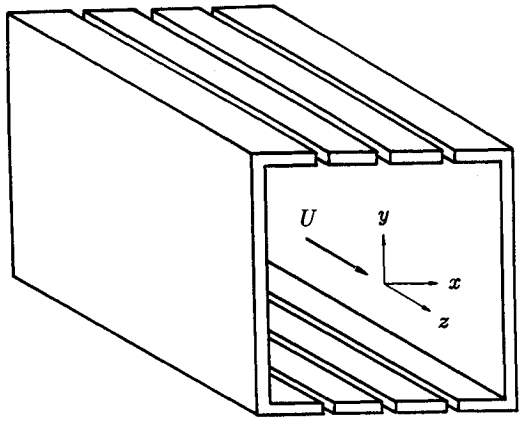

Fig. 1 Rectangular tunnel with slotted roof and floor.

When

$$(M\omega/U) < \beta\Lambda_n \tag{11}$$

then α has two conjugate complex values, and Eq. (2) is no longer a traveling wave of constant amplitude.

For each eigenvalue Λ_n, the smallest value of ω for which a disturbance of Eq. (2) can have bounded amplitude is given by

$$\omega = \omega_r = (\beta/M)U\Lambda_n \tag{12}$$

For the preceding condition, we get the following relation from Eq. (9):

$$\alpha = M^2\omega/U\beta^2 \tag{13}$$

Substituting Eq. (13) into (3), we can obtain the following equation:

$$\Phi_{xx} + \Phi_{yy} + (\omega/a_0\beta)^2\Phi = 0 \tag{14}$$

When Eq. (2) is substituted, Eq. (14) is equivalent to the following equation:

$$\phi_{xx} + \phi_{yy} - (1/a_0\beta)^2\phi_{tt} = 0 \tag{15}$$

This is the wave equation with the effective speed of sound

$$a_e = a_0\beta = a_0\sqrt{1 - M^2} \tag{16}$$

The effective speed of sound is illustrated in Fig. 2. Perturbation pressure is computed from the following relation, consistent with Eq. (1):

$$p = -\rho\left(\frac{\partial\phi}{\partial t} + U\frac{\partial\phi}{\partial z}\right) \tag{17}$$

From Eq. (2), pressure is given by

$$p = -i\rho(\omega + \alpha U)\phi \tag{18}$$

Using Eq. (18), we can then derive the following equation from Eq. (15):

$$p_{xx} + p_{yy} + (\omega/a_e)^2 p = 0 \tag{19}$$

This is the two-dimensional Helmholtz equation with the effective speed of sound a_e. Therefore, we can consider our problem as a two-dimensional acoustic system in which the speed of sound is a_e. This equation will be used to obtain the resonant frequencies in a later section.

On the rigid boundary, it follows from Eqs. (4) and (18)

$$\frac{\partial p}{\partial n} = 0 \tag{20}$$

where n is again the outward normal to the boundary.

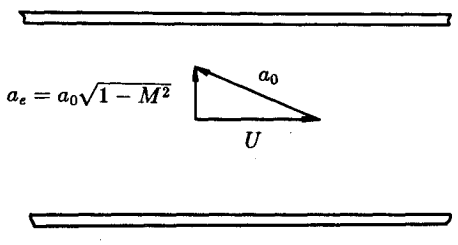

Fig. 2 Effective speed of sound.

III. Variational Principle for Wind Tunnel System

The calculus of variations is a reliable guide both for formulating and solving differential equations of mathematical physics.[10] Variational principles have been used in various fields, such as dynamics, structures, and continuum mechanics. Recently they were applied to acoustic problems and to the interaction between acoustics and structures.[11-22] Gladwell[23,24] gives the energy and complementary energy formulations of acoustic and structural vibration systems. In treating dynamics problems, Hamilton's principle is one of the most useful and important variational statements.

Hamilton's principle considers the entire motion of the system between two instants t_0 and t_1, and it is therefore an integral principle. The problems of dynamics are reduced to the investigation of a scalar integral. Hamilton's principle reads

$$\delta \int_{t_0}^{t_1} L \, dt = 0 \tag{21}$$

This principle states that, between two instants of time t_0 and t_1, the motion is such that the integral of the Lagrangian function is stationary for the actual motion when compared with all other possible motions taking on the prescribed actual values at t_0 and t_1.

The function $\boldsymbol{B}$ is a linear function of the displacements if the external pressures are independent of the displacement. If the external pressures depend on the time history of the displacement, we should use the following variational form:

$$\int_{t_0}^{t_1} \delta(U - T - B) \, dt = 0 \tag{22}$$

If the external pressure does not depend on the time history of the displacement, this equation becomes Eq. (21) and the Lagrangian function L can be written as

$$L = U - T - B = \frac{1}{2}\int_V \rho a_e^2 (\nabla \cdot \xi)^2 \, dv - \frac{1}{2}\int_V \rho \left(\frac{\partial \xi}{\partial t}\right)^2 dv - \int_{S_2} (-p)\xi_n \, ds \tag{23}$$

Here, a_e is used instead of a_0 because our wind-tunnel system can be considered to have this effective speed of sound.

We will follow Gladwell's procedure[23] to obtain the variational functional for the wind tunnel resonance problem. If we are interested primarily in harmonic vibration problems in which all displacements, forces, pressures, etc., have time-dependence $e^{i\omega t}$, such problems may be formulated entirely in terms of the time-independent amplitudes. For such problems, Hamilton's principle may be replaced by a simpler time-independent principle.[23]

Suppose that the boundary surface S is divided into two parts S_1 and S_2 with the following boundary conditions: displacement ξ is specified on S_1 and pressure p is specified on S_2. For the wind-tunnel system, which is in harmonic motion, the constitutive equation is

$$p = -\rho a_e^2 \nabla \cdot \xi \tag{24}$$

The dynamic equilibrium equation is

$$-\rho\omega^2 \xi = -\nabla p \tag{25}$$

Then, the principle of stationary energy reads

$$\delta L = 0 \tag{26}$$

where

$$L = U - T - B = \frac{\rho a_e^2}{2}\int_V (\nabla \cdot \xi)^2 \, dv - \frac{\rho\omega^2}{2}\int_V \xi^2 \, dv - \int_{S_2} (-p)\xi_n \, ds \tag{27}$$

Here, the variational displacements are arbitrary only on the surface S_2 where pressures are specified.

A. Principle of Stationary Complementary Energy

Since structural vibration problems are usually formulated in terms of displacements, whereas acoustic vibration problems involve the pressure (a forcelike quantity), it is necessary to recast the functional in terms of the pressure for Eq. (27). Alternatively, we can formulate a complementary variational principle for the acoustic pressure by considering the complementary virtual work. We assume that the medium is in the linear elastic range. Therefore, the complementary potential energy, kinetic energy, and work done on the boundary are equal to those given in Eq. (27).

The time-independent complementary principle can be formulated by substituting Eqs. (24) and (25) into Eq. (27). Then, the time-independent functional is

$$F = U_c - T_c - B_c = \frac{1}{2\rho a_e^2}\int_V p^2 \, dv - \frac{1}{2\rho\omega^2}\int_V (\nabla p)^2 \, dv + \int_{S_1} p\xi_n \, ds \tag{28}$$

where ξ_n is the amplitude of the specified displacement. Here, the complementary potential energy U_c and kinetic energy T_c are expressed in terms of pressure, and B_c is such that its variation gives the work done by the virtual pressure over the boundary. The variational pressures are arbitrary only on the surface S_1 where displacements are specified.

One sees that the principle of stationary complementary energy[23] involves forcelike quantities. This principle states that of all pressures satisfying the specified boundary conditions, that which satisfies the constitutive and equilibrium equations and the remaining kinematic boundary conditions is determined by the variational equation

$$\delta F = 0 \tag{29}$$

We will use the principle of stationary complementary energy to solve the wind-tunnel resonance problem for arbitrary boundaries.

B. Variational Functional for Closed and Open Wind Tunnels

The equation for an acoustic system without any energy dissipation at the boundaries is obtained from the variation of Eq. (28). When there is no work done on the boundary, the appropriate functional for a closed and open wind tunnel can be written as

$$F = \frac{1}{2\rho a_e^2}\int_V p^2 \, dv - \frac{1}{2\rho\omega^2}\int_V (\nabla p)^2 \, dv \tag{30}$$

Here, a_e is again the effective speed of sound as given in Eq. (16). Setting the first variation of this functional F to zero leads to the Helmholtz equation

$$\nabla^2 p + (\omega^2/a_e^2)p = 0 \tag{31}$$

and the boundary condition on the solid wall is

$$\frac{\partial p}{\partial n} = 0 \tag{32}$$

where n is the outward normal to the surface. These are the correct governing equations and boundary condition. Hence, we will use the functional in Eq. (30) as the starting point for the finite-element solution.

IV. Finite-Element Formulation

Within each element v_i, we can approximate the pressure distribution by the row matrix $\lfloor N \rfloor_i$ of shape functions

$$p = \lfloor N \rfloor_i \{p\}_i \tag{33}$$

Here, $\{p\}_i$ is a column vector of nodal pressure values for this ith element.

For each element, the potential energy of the subvolume v_i can be written as

$$U_i = \frac{1}{2\rho a_e^2} \int_{v_i} p^2 \, dv = \frac{1}{2\rho} \{p\}_i^T [k]_i \{p\}_i \tag{34}$$

where the stiffness matrix $[k]_i$ is

$$[k]_i = \int_{v_i} \frac{1}{a_e^2} \lfloor N \rfloor_i^T \lfloor N \rfloor_i \, dv \tag{35}$$

The kinetic energy of the subvolume v_i can be written as

$$T_i = \frac{1}{2\rho\omega^2} \int_{v_i} (\nabla p)^2 \, dv = \frac{1}{2\rho\omega^2} \{p\}_i^T [m]_i \{p\}_i \tag{36}$$

where the mass matrix $[m]_i$ is

$$[m]_i = \int_{v_i} [B]_i^T [B]_i \, dv \tag{37}$$

where

$$[B]_i = \begin{Bmatrix} \dfrac{\partial}{\partial x} \\ \dfrac{\partial}{\partial y} \\ \dfrac{\partial}{\partial z} \end{Bmatrix} \lfloor N \rfloor_i \tag{38}$$

Therefore, for each element, we can get the functional F_i from Eq. (30)

$$F_i = \frac{1}{2\rho\omega^2} (\omega^2 \{p\}_i^T [k]_i \{p\}_i - \{p\}_i^T [m]_i \{p\}_i) \tag{39}$$

The first variation of Eq. (39) gives the following eigenvalue problem for subvolume v_i:

$$[m]_i \{p\}_i - \omega^2 [k]_i \{p\}_i = \{0\} \tag{40}$$

If we assemble the subelements in the standard fashion for finite-element formulations, we get the eigenvalue problem for the complete volume V

$$([M] - \omega^2 [K]) \{p\} = \{0\} \tag{41}$$

where $[M]$ is the mass matrix for the complete system and $[K]$ is the stiffness matrix for the complete system.

For this analysis, isoparametric finite-element matrices are used. In most practical analyses, the use of an isoparametric finite element is more effective.[25] Two-dimensional four-node elements are used to calculate element mass and stiffness matrices. Two-dimensional elements only are needed to solve the wind-tunnel resonance problem because, in general, the wind-tunnel cross section can be assumed to be two-dimensional.

V. Results and Discussion

A. Convergence of Two-Dimensional Isoparametric Elements

The requirements for monotonic convergence of the finite-element analysis are compatibility and completeness. The isoparametric element formulation with the appropriate interpolation functions satisfies these convergence criteria.[25]

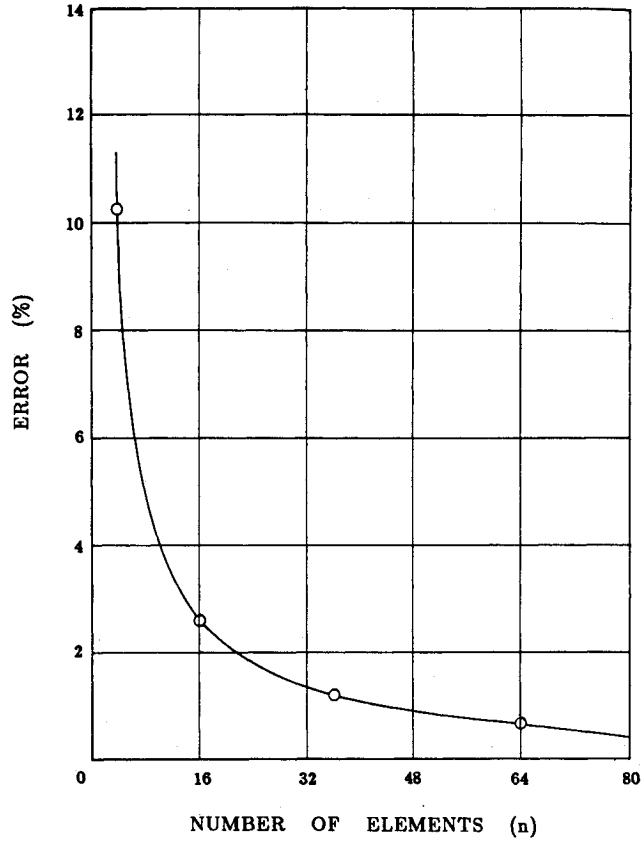

Fig. 3 Convergence rate of finite-element results for rectangular cross section.

In this section, to examine the convergence rate, the resonant frequency for a rectangular tunnel was obtained by the finite-element method when the slots are closed. This case has an exact solution for comparison. The more elements that are used, the better the finite-element results will approach that exact solution.

Let us define the nondimensional resonant frequency α_f as

$$\alpha_f = \frac{\omega H}{\beta a_0}$$

The exact value of α_f is π for the fundamental acoustic mode. This value is given by Acum.[6] For the slot-closed case, the convergence rate of finite-element results for the fundamental frequency is illustrated in Fig. 3. If we choose $n = 40$, then the estimate will be approximately 1% higher than the exact value.

B. Wind Tunnel with Rectangular Cross Section

Many wind tunnels have slots on the wall of the test section to reduce the blockage effect of the model inserted in the section. It was found many years ago that the resonant frequency is affected by the ratio of open to closed area.[6,26] In this section, we will discuss the results of the resonant frequency calculations for a rectangular tunnel with slots on the wall.

Rectangular Tunnel with One Slot

Let us first consider the rectangular tunnel with one slot in each floor, as shown in Fig. 4. The slot width is d. The tunnel height is H. We define the open area ratio e as

$$e = d/H$$

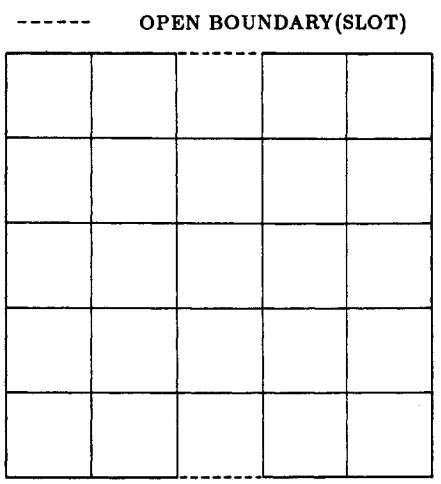

Fig. 4 Rectangular cross section with one slot each on roof and floor.

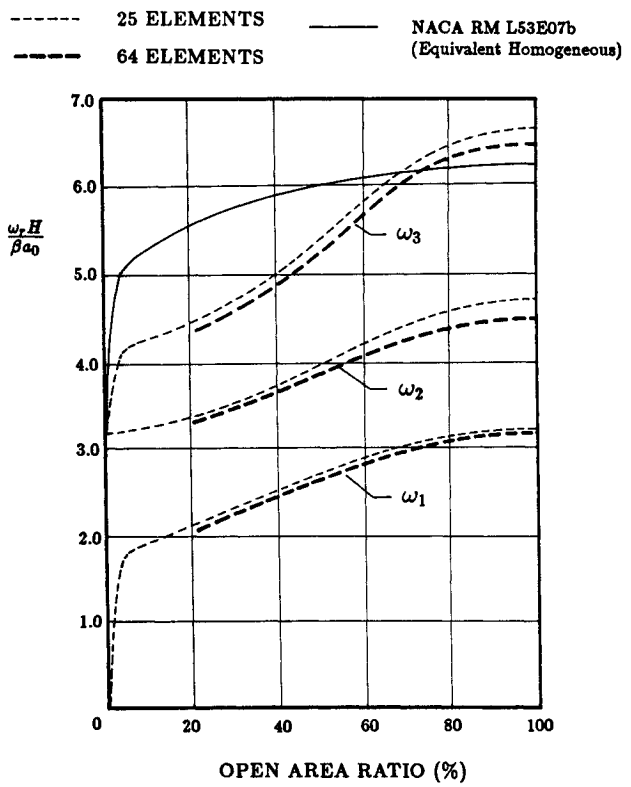

Fig. 5 First three resonant frequencies for rectangular cross section with one slot each on roof and floor.

For a slotted tunnel, the resonant frequency can be obtained by applying the boundary condition at the slotted portion of the wall ($p = 0$). The finite-element results are given in Fig. 5. They are obtained using both 25 and 64 elements. The convergence rate is very fast. The solid curve is taken from Davis and Moore's result,[26] which was obtained by assuming an averaged homogeneous boundary condition. As the open area increases, the resonant frequency increases. The first frequency ω_1 corresponds to the symmetrical mode shape with respect to the vertical and horizontal centerline. If the wind-tunnel model is installed horizontally in the centerline of the wind tunnel, this mode shape will not couple with model oscillation. The second frequency ω_2 corresponds to the mode shape that has as a node line the vertical centerline of the wind-tunnel cross section. This

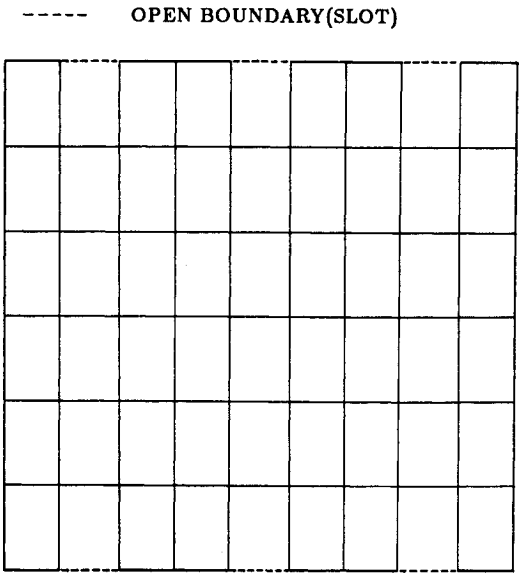

Fig. 6 Rectangular cross section with three slots each on roof and floor.

mode shape is the horizontal vibrational mode. Therefore, if the wing is installed horizontally, this mode shape is not important. The third frequency ω_3 corresponds to the mode shape whose node line is the horizontal centerline. Therefore, this frequency is important when the wind-tunnel model is horizontally installed because of a very strong coupling. This horizontal installation is the common arrangement for aeroelastic model testing.

Rectangular Tunnel with Three Slots

Many wind tunnels have several slots in the top and bottom boundaries. Several slots will be more effective in reducing the distortion of streamlines in the test section. Let us consider a three-slotted wind tunnel, as shown in Fig. 6. In this case, the open area ratio e is $3d/H$. The finite-element results are given in Fig. 7. The first frequency ω_1 corresponds to the symmetrical mode shape with respect to the vertical and horizontal centerlines. The second frequency ω_2 corresponds to the horizontal vibration mode. The third frequency ω_3 again has as its node the horizontal centerline. The solid curves were obtained by the substitution of an equivalent homogeneous boundary for the discrete slots,[26] as explained in the previous section. For 81 elements, ω_3 is approximately 2% higher than that obtained by Davis and Moore.[26] The resonant frequencies of a wind tunnel with three slots (Fig. 7) are much smaller than those with one slot (Fig. 5) at the same open area ratio. For a slotted wind tunnel, more elements are required than in the closed tunnel case for a given level of accuracy. If we consider the slot thickness in the finite-element formulation, the smaller elements will obviously give relatively accurate results. NASA Ames 6 ft × 6 ft tunnel is a rectangular tunnel with five slots. The resonant frequencies of this tunnel will be very close to the frequencies of the tunnel with three slots.

C. Wind Tunnel with Octagonal Cross Section

NASA Langley Research Center operates the 16 ft × 16 ft transonic dynamics tunnel. Its cross-sectional shape is octagonal. For this kind of tunnel, the analytical approach does not calculate the resonant frequency accurately. In this case, the finite-element method is a useful method. The octagonal cross-section shape can be modeled by using quadrilateral finite elements, and this is shown in Fig. 8.

The Boeing supersonic transport (SST) model was tested at NASA Langley to investigate the effect of the wind-tunnel resonance on the flutter, and the experimental results are given by Ruhlin, Destuynder, and Gregory.[27] The NASA Langley tran-

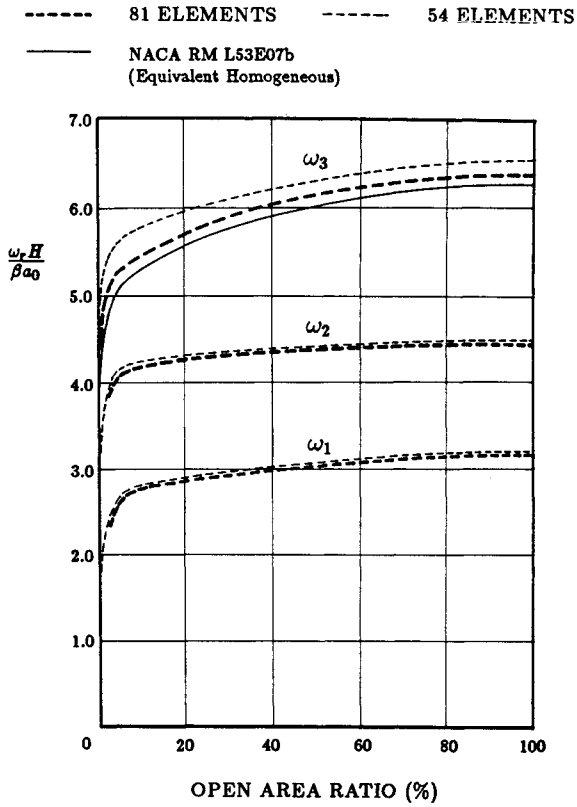

Fig. 7 First three resonant frequencies for rectangular cross section with three slots each on roof and floor.

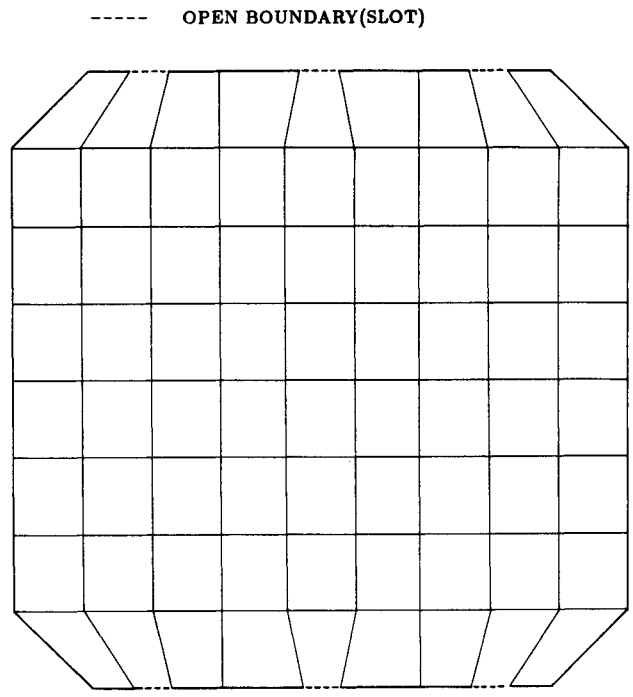

Fig. 8 Octagonal cross section of NASA Langley 16 ft × 16 ft transonic dynamics tunnel.

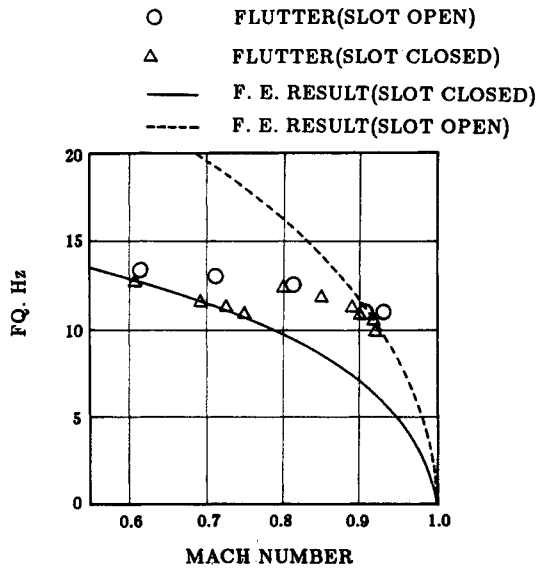

Fig. 9 Resonant frequency and experimental flutter results for SST wing model in NASA Langley 16 ft × 16 ft transonic dynamics tunnel.

sonic dynamics tunnel has a fixed porosity value of 4.2%, and the sidewall also has about the same porosity. During this test, the sidewall slots were closed and both top and bottom slots were open. Freon gas was used as the fluid medium, in which the speed of sound is 498.7 ft/s. The finite-element results for the resonant frequencies and the model flutter results are given in Fig. 9. When the slots are closed, the tunnel resonant frequencies are close to the model flutter frequencies in the Mach number range from 0.6 to 0.75. Thus, it was concluded that the proximity of the tunnel resonant frequency to the flutter frequency near $M = 0.6$ to 0.75 was the likely cause for the lower flutter speeds with the slots' closed condition.[27] This feature is also shown in Fig. 10. A solid curve represents the analytical free-air analysis for the flutter.[27] Triangular symbols correspond to the flutter test results for the slot-closed condition and circles to the slot-open condition.

D. Mode Shapes

The eigenvectors are obtained for both the rectangular and the octagonal cross-section wind tunnel to investigate the mode shapes.

Rectangular Tunnel

The mode shapes for a rectangular cross-section wind tunnel with closed slots are given in Fig. 11. The first frequency is zero, and all the eigenvectors have the same values. Therefore, there is no relative motion in the x-y plane. The second and third resonant frequencies are the same. For the second resonant frequency, the node line is vertical. Therefore, this mode corresponds to the horizontal vibration mode. For the third resonant frequency, the node line is horizontal and this mode corresponds to the vertical vibration mode. Hence, for the common case of a model installed horizontally, the third resonant frequency is important. It should be noted that $\partial p/\partial n$ at the solid wall is zero. To investigate the eigenvectors for this rectangular tunnel, 54 elements were used in this case.

Octagonal Tunnel

Figure 12 shows the mode shapes of the NASA Langley 16 ft × 16 ft transonic dynamics tunnel when the slots are closed. For this analysis, 72 elements were used. The mode shapes are similar to those of the rectangular tunnel, but in this case the pressure variations along each horizontal line parallel to the x axis have slightly different values due to the corner effect. The maximum variation of pressure is in the x axis (section 1 in Fig. 12a). The second frequency corresponds to that of the horizontal vibration mode. The third frequency corresponds to the vertical vibration mode for which the nodal line is the horizontal centerline. The mode shapes are the same as the horizontal vibration mode shapes.

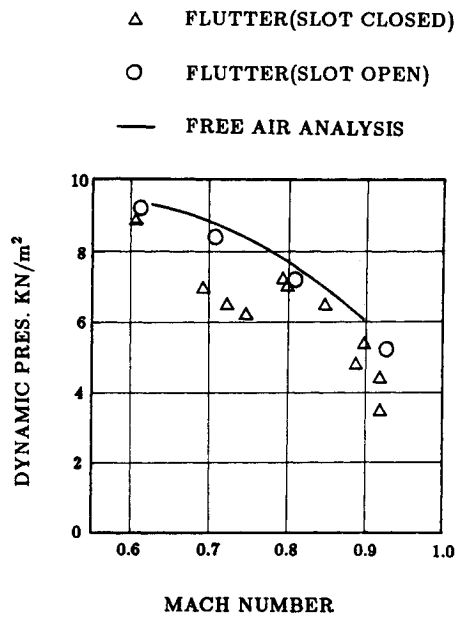

Fig. 10 Experimental and analytical flutter results for SST wing model in NASA Langley 16 ft × 16 ft transonic dynamics tunnel.[27]

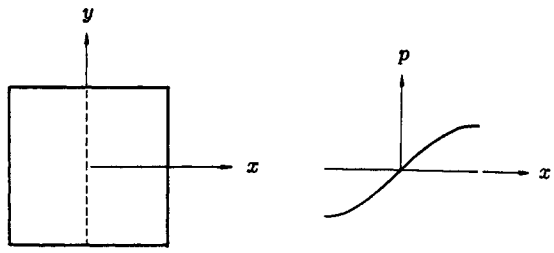

a) Horizontal vibration mode, $\omega = \omega_2$

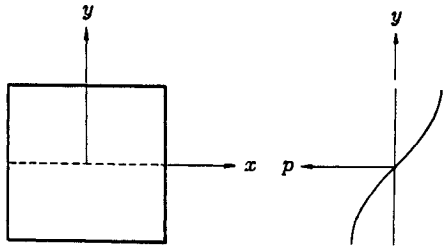

b) Vertical vibration mode, $\omega = \omega_3$

Fig. 11 Mode shapes of rectangular cross section with closed slot.

Summary

A finite-element approach to obtain the resonant frequency of the wind tunnel with an arbitrarily shaped cross section was developed that gave very accurate results. The convergence rate of finite-element results was given for a slot-closed case. With 50 finite elements, the error for a rectangular wind tunnel is within 1% of the exact value. The resonant frequencies of rectangular wind tunnels were obtained. The resonant frequencies of a wind tunnel with one slot are much smaller than those of a tunnel with three slots. Also, the frequencies for an octagonal cross section were obtained.

Acknowledgments

This research was performed under NASA Grant NGL-05-020-243. The author wishes to express his appreciation to Professor H. Ashley for valuable discussions with him.

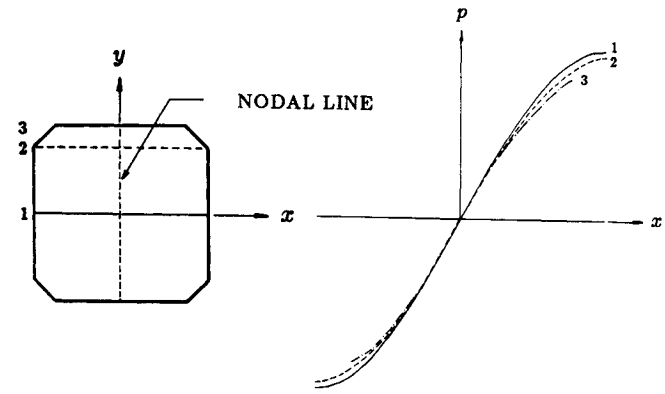

a) Horizontal vibration mode, $\omega = \omega_2$

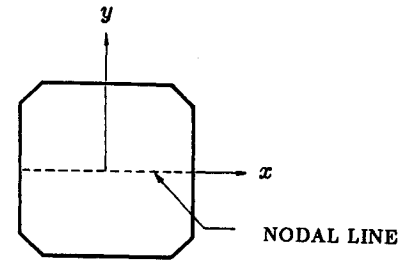

b) Vertical vibration mode, $\omega = \omega_3$

Fig. 12 Mode shapes of NASA Langley transonic dynamics tunnel with closed slot.

References

[1]Widmayer, E., Clevenson, S. A., and Leadbetter, S. A., "Some Measurements of Aerodynamic Forces and Moments at Subsonic Speeds on a Rectangular Wing of Aspect Ratio 2 Oscillating About the Midchord," NACA TN 4240, 1958.

[2]Clevenson, S. A. and Widmayer, E., "Experimental Measurements of Forces and Moments of a Two-Dimensional Oscillating Wing at Subsonic Speeds," NACA TN 3686, 1956.

[3]Runyan, H. L. and Watkins, C. E., "Considerations on the Effect of Wind-Tunnel Walls on Oscillating Air Forces for Two-Dimensional Subsonic Compressible Flow," NACA Rept. 1150, 1953.

[4]Runyan, H. L., Woolston, D. S., and Rainey, A. G., "Theoretical and Experimental Investigation of the Effect of Tunnel Walls on the Forces on an Oscillating Airfoil in Two-Dimensional Subsonic Compressible Flow," NACA Rept. 1262, 1956.

[5]Jones, W. P., "Wind-Tunnel Wall Interference Effects on Oscillating Aerofoils in Subsonic Flow," Aeronautical Research Council, Rept. and Memo 2943, 1953.

[6]Acum, W. E. A., "A Simplified Approach to the Phenomenon of Wind Tunnel Resonance," Aeronautical Research Council, Rept. and Memo 3371, 1962.

[7]Acum, W. E. A., "Subsonic Wind Tunnel Wall Corrections," AGARD-ograph 109, 1966, Chap. 4.

[8]Rushton, K. R., "Studies of Slotted-Wall Interference Using an Electrical Analogue," Aeronautical Research Council, Rept. and Memo 3452, 1965.

[9]Garner, H. C., Moore, A. W., and Wight, K. C., "The Theory of Interference Effects on Dynamic Measurements in Slotted-Wall Tunnels at Subsonic Speeds and Comparisons with Experiment," Aeronautical Research Council, Rept. and Memo 3500, 1966.

[10]Courant, R. and Hilbert, D., *Methods of Mathematical Physics*, Wiley-Interscience, New York, 1953.

[11]Gladwell, G. M. L., "A Finite Element Method for Acoustics," *Proceedings of the 5th International Congress on Acoustics*, Paper L. 33, Sept. 1965.

[12]Graggs, A., "The Transient Response of a Coupled Plate Acoustic System Using Plate and Acoustic Finite Elements," *Journal of Sound and Vibration*, Vol. 15, April 1971, pp. 509–528.

[13]Craggs, A., "The Use of Simple Three-Dimensional Acoustic Finite Elements for Determining the Natural Modes and Frequencies of Complex Shaped Enclosures," *Journal of Sound and Vibration*, Vol. 23, No. 3, Aug. 1972, pp. 331–339.

[14]Craggs, A., "An Acoustic Finite Element Approach for Studying Boundary Flexibility and Sound Transmission Between Irregular Enclosures," *Journal of Sound and Vibration*, Vol. 30, No. 3, Oct. 1973, pp. 343–357.

[15]Herting, D. N., Joseph, J. A., Kuusinen, L. R., and MacNeal, R. H., "Acoustic Analysis of Solid Rocket Motor Cavities by a Finite Element Method," NASA TM X-2378, 1971, pp. 285–324.

[16]Petyt, M., Lea, J., and Koopmann, G. H., "A Finite Element Method for Determining the Acoustic Modes of Irregular Shaped Cavities," *Journal of Sound and Vibration*, Vol. 45, April 1976, pp. 495–502.

[17]Shuku, T. and Ishihara, K., "The Analysis of the Acoustic Field in Irregularly Shaped Rooms by the Finite Element Method," *Journal of Sound and Vibration*, Vol. 29, No. 1, July 1973, pp. 67–76.

[18]Young, C. J. and Crocker, M. J., "Prediction of Transmission Loss in Mufflers by the Finite Element Method," *Journal of Acoustical Society of America*, Vol. 57, Jan. 1975, pp. 144–148.

[19]Ross, D. F., "A Finite Element Analysis of Parallel-Coupled Acoustic Systems Using Subsystems," *Journal of Sound and Vibration*, Vol. 69, April 1980, pp. 509–518.

[20]Young, C. J., "Acoustic Analysis of Mufflers for Engine Exhaust Systems," Ph.D. Dissertation, Purdue Univ., Lafayette, IN, 1973.

[21]Unruh, J. F., "Finite Element Subvolume Technique for Structural-Borne Interior Noise Prediction," *Journal of Aircraft*, Vol. 17, June 1980, pp. 434–441.

[22]Unruh, J. F., "Structural-Borne Noise Prediction for a Single-Engine General Aviation Aircraft," *Journal of Aircraft*, Vol. 18, Aug. 1981, pp. 687–694.

[23]Gladwell, G. M. L. and Zimmermann, G., "On Energy and Complementary Energy Formulations of Acoustic and Structural Vibration Problems," *Journal of Sound and Vibration*, Vol. 3, No. 3, May 1966, pp. 233–241.

[24]Gladwell, G. M. L., "A Variational Formulation of Damped Acousto-Structural Vibration Problems," *Journal of Sound and Vibration*, Vol. 4, No. 2, Sept. 1966, pp. 172–186.

[25]Bathe, K.-J. and Wilson, E. L., *Numerical Methods in Finite Element Analysis*, Prentice-Hall, Englewood Cliffs, NJ, 1976.

[26]Davis, D. D. and Moore, D., "Analytical Study of Blockage- and Lift-Interference Corrections for Slotted Tunnels Obtained by the Substitution of an Equivalent Homogeneous Boundary for the Discrete Slots," NACA Research Memo L53E07b, June 1953.

[27]Ruhlin, C. L., Destuynder, R. M., and Gregory, R. A., "Some Tunnel Wall Effects on Transonic Flutter," AIAA Paper 74-406, April 1974.